Advances in Geo-Energy Research

Vol. 13, No. 1, p. 10-21, 2024

Original article

Mechanism of organo-nickel co-enrichment in marine black shale

Peng Xia[1,2,3]*, Fang Hao[3], Cong Yang[1,2], Jinqinag Tian[3], Yong Fu[1,2], Ke Wang[1,2]

[1]*Resource and Environmental Engineering College, Guizhou University, Guiyang 550025, P. R. China*
[2]*Key Laboratory of Ministry of Education for Geological Resources and Environment, Guiyang 550025, P. R. China*
[3]*School of Geosciences, China University of Petroleum (East China), Qingdao 266580, P. R. China*

Keywords:
Geochemistry
black shale
organic matter
clay minerals
nickel
paleoenvironment

Cited as:
Xia, P., Hao, F., Yang, C., Tian, J., Fu, Y., Wang, K. Mechanism of organo-nickel co-enrichment in marine black shale. Advances in Geo-Energy Research, 2024, 13(1): 10-21.
https://doi.org/10.46690/ager.2024.07.03

Abstract:
Organic matter and metal elements are commonly co-enriched in marine black shales. However, the element types vary among different shales and the relevant mechanisms of organo-metal co-enrichment are still unclear. The super-enrichment of organic matter and nickel in the ore bed of Early Cambrian marine black shale of southern China provides an ideal opportunity to investigate this mechanism. Herein, to clarify the co-enrichment mechanism of organic matter and , the laminated structure of this ore bed was characterized and the geochemical and mineralogical proxies of different laminae were analyzed. The results indicated that there are four types of laminae in this ore bed, namely, siliceous laminae, calcareous laminae, clay minerals laminae, and organic-rich laminae. Clay minerals laminae and organic-rich laminae were deposited under anoxic environments, while siliceous laminae were deposited under strong oxidizing to anoxic environments. Neither organic matter nor are distributed homogeneously in the ore bed; organic matter is mainly concentrated in organic-rich laminae, while is largely enriched in clay minerals laminae. Clay minerals and organic matter have strong adsorption capacity for , and the adsorption capacity of clay minerals (such as illite) for is stronger than that of organic matter. Hydrothermal events and terrestrial input are key factors affecting the paleoenvironment and laminated structure during the deposition of the ore bed. Although organic matter and are co-enriched in the ore bed, their enrichment stages and conditions vary according to the geochemical differences among laminae.

1. Introduction

Black shales, primarily developed during certain periods of geological history, not only record the changes in the paleoenvironment and paleoclimate, as well as provide paleontological data but also contain large quantities of metal-rich minerals and oil/gas resources (Hao et al., 2011, 2013; Shi et al., 2021; Laranjeira et al., 2023; Li and Cai, 2023; Zhao et al., 2024). Early Cambrian black shale in the Upper Yangzte Region is an iconic deposit dating from the Neoproterozoic to the Early Paleozoic Era in southern China, which corresponds to the fragmentation and aggregation of the supercontinent, the turbulent changes in marine chemistry and biochemistry, and the episodic replacement of life (Hoffman et al., 1998; Och et al., 2013; Zhang et al., 2014; Guizhou Geological Survey, 2017; Zhu et al., 2019a; Xia et al., 2022). This black shale contains 3.55×10^{12} m^3 (125.37 tcf) shale gas in Guizhou Province alone and is rich in metal elements, such as nickel (Ni), vanadium (V), molybdenum (Mo), uranium (U), and those of the platinum group (PGE) (Fan et al., 2004; Mou et al., 2024).

In Early Cambrian black shale, the spatial distribution of organic matter and metal elements, especially , is closely related. For example, the abundance of organic matter in the ore bed is significantly higher than that in the black shale outside the ore bed (Han et al., 2015; Ning et al., 2022; Xia et al., 2022). In this ore bed, occurs as independent minerals, isomorphic complexes, and in adsorbed state (Pan et al., 2005;

Yandy Scientific Press

*Corresponding author.
E-mail address: pxia@gzu.edu.cn (P. Xia); haofang@cup.edu.cn (F. Hao); 15186945585@163.com (C. Yang); tianjq@cup.edu.cn (J. Tian); byez1225@126.com (Y. Fu); kwang5@gzu.edu.cn (K. Wang).

Received March 19, 2024; revised April 11, 2024; accepted May 3, 2024; available online May 8, 2024.

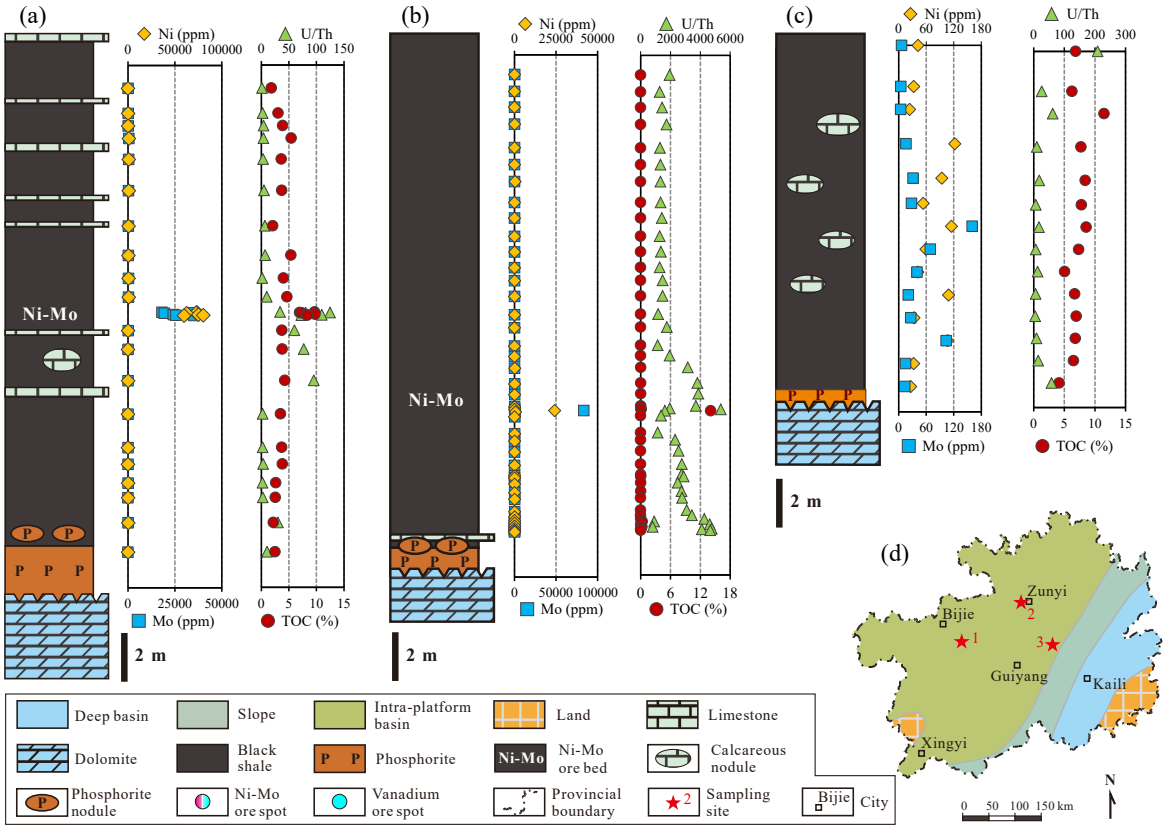

Fig. 1. Geochemical characteristics of Early Cambrian black shale sections (the geochemical data was partly cited from Pi et al. (2013); Han et al. (2015); Xia et al. (2022)). (a) Yulongba section, (b) Songlin section, (c) Yonghe section and (d) locations of these sections.

Han et al., 2012; Cao et al., 2013; Shi et al., 2014; Yu et al., 2023). The occurrence states of organic matter in the ore bed include banded, masses, filled, and mutual wrapped types (Zhang et al., 2017; Yu et al., 2022). The distribution of and organic matter in the ore bed is heterogeneous and their relationship is unknown. Fortunately, this ore bed has been revealed to exhibit laminated structure according to previous researches and our existing work (Mao et al., 2002; Han et al., 2015, 2020; Lehmann et al., 2016; Yu et al., 2022). Thus, based on the differences in geochemical characteristics among various laminae, the environmental evolution and enrichment process of Ni and organic matter during the deposition of this ore bed can be readily investigated. Previous works to reconstruct paleoenvironment of the Early Cambrian Niutitang Formation were based on powdered samples of total rock, and they were limited to reflecting the sedimentary evolution based on in-situ geochemical data. These powder samples were obtained from different layers with thickness no less than 0.1 m. The reconstructed models can reflect millennial scale changes, but they fail to reconstruct decadal scale changes in the paleoenvironment. In-situ geochemical analysis of laminae can be employed to indicate the environmental change from seasonal to decadal (Liang et al., 2018; Xin et al., 2022), which will contribute to investigating the mechanism of organo-metal co-enrichment in Early Cambrian marine black shale.

The primary goal of this study was to determine the characteristics and types of laminae in the Ni ore bed from Early Cambrian marine black shale. Subsequently, the geochemical characteristics and environmental evolution were described, and a mechanistic model of organo-metal co-enrichment were built. The findings enhance our understanding of the co-enrichment mechanism of organo-metal in marine black shale, and serve as a guide to shale gas exploration and development.

2. Materials and methods

2.1 Sample collection and preparation

A total of 32 black shale samples were collected from two sections for geochemical analyses. Among these, 18 samples were obtained from the Songlin section and 14 samples were from the Yonghe section (Fig. 1). First, all the potentially weathered surfaces, visible pyrite grains, and post-depositional veins were removed from each sample. Then, the samples were cut into small pieces. One piece of each sample was selected to grind into thin slices, and approximately 100 g of fresh pieces was crushed to powder (> 200 mesh) using a tungsten carbide crusher.

2.2 Analytical methods

The samples were acidified using 5% HCl to remove the carbonates and neutralized to pH = 7.0 by adding deionized water, followed by the measurement of total organic carbon

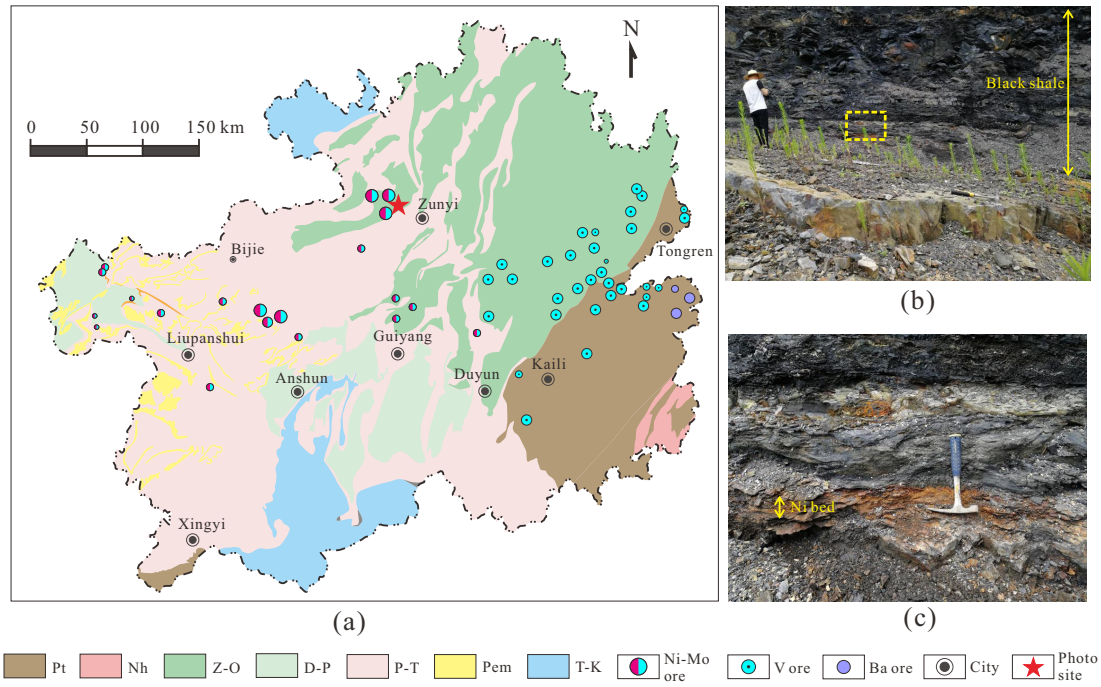

Fig. 2. Geological map (a) and field photos of Niutitang black shale (b) and the Ni ore bed (c) in it. Photo (c) represents the yellow dashed box in photo (b). Pt: Proterozoic; Nh: Nanhua; Z: Edicaran; O: Ordovician; D: Devonian; P: Permian; T: Triassic; Pem: Emeishan basalt; K: Cretaceous.

(TOC) content and concentration of trace elements in all sample powders. The TOC content of powder samples was determined at Guizhou University using a LECO CS-230 sulfur-carbon analyzer. The analysis of trace element concentrations in the powdered samples was conducted at China University of Petroleum using an inductively coupled plasma mass spectrometer. The data of shale samples from Yulongba and Songlin sections reported in previous researches were also cited.

The laminae of thin slice samples were observed and their composition was determined using a Zeiss optical microscope at Guizhou University. In total, the trace element concentrations of 55 laminae were measured, and the analyses of in-situ trace element concentrations were conducted using a laser ablation inductivity coupled plasma mass spectrometer (LA-ICP-MS) at the Institute of Geochemistry, Chinese Academy of Science. During the LA-ICP-MS analyses, the wavelength and spot size of laser were 193 nm and 4-160 μm, respectively.

3. Results and discussion

3.1 Geochemical differences between ore bed and its surrounding black shale

The bottom layer of Early Cambrian Niutitang Formation in Guizhou Province is black shale with a thickness of 20-120 m, characterized by high TOC content (range of 0.7%-14.6%, with an average of 5.2%), high to over mature organic matter (vitrinite reflectance, Ro, is 1.4%-4.9%), and the enrichment of critical metallic elements, including , V, Mo, U, and PGE (Han et al., 2020; Shi et al., 2021; Mou et al., 2024). Specifically, is enriched to form an ore bed in Northwest Guizhou (Figs. 1 and 2), with an intra-platform basin during deposition (Dai et al., 2013; Guizhou Geological Survey, 2017; Xia et al., 2022). The thickness of the ore bed is generally less than 0.1 m, which forms only a small portion of the Early Cambrian black shale. However, the geochemical characteristics of this ore bed are significantly different from the black shale outside of it (Fig. 1).

As shown in Fig. 1, in contrast to black shale, the ore bed has much higher TOC content, ranging from 6.94% to 16.10% with an average value of 9.48%, while the TOC content in the black shale outside this ore bed is 1.80%-12.60% and the average value is 4.80%. The concentrations in the ore bed and black shale are 36,194.0-70,292.0 ppm (averaging 50,504.6 ppm) and 15.6-869.0 ppm (averaging 174.2 ppm), respectively. These figures imply that element and organic matter are co-enriched in Early Cambrian black shale.

Apart from TOC content and Ni concentration, the paleo-environmental proxies of Ni ore bed are also different from those of black shale. Redox-sensitive elements (such as U, Ni, Mo, V, Co and Cr) and their ratios (mainly including U/Th, U/Mo, V/(V+), V/Cr, and /Co) can indicate paleoredox conditions. It is noteworthy that and Mo are abnormally enriched in the ore bed, so U/Th and V/Cr were calculated, indicating paleoredox conditions. The U/Th and V/Cr ratios of black shale are in the range of 1.23-190.16 and 0.41-70.00, respectively. In contrast to black shale, Ni ore samples have higher U/Th value (33.94-124.71) and lower V/Cr value (0.97-

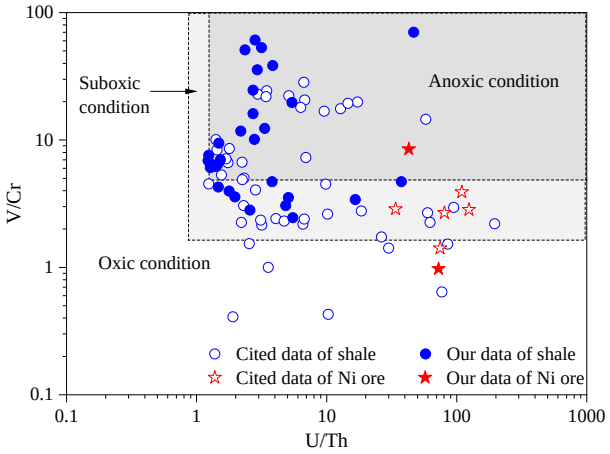

Fig. 3. Cross-plot of V/Cr and U/Th indicating paleoredox conditions (the data with hollow circles and five-pointed stars are cited from Pi et al. (2013); Han et al. (2015); Xia et al. (2022)).

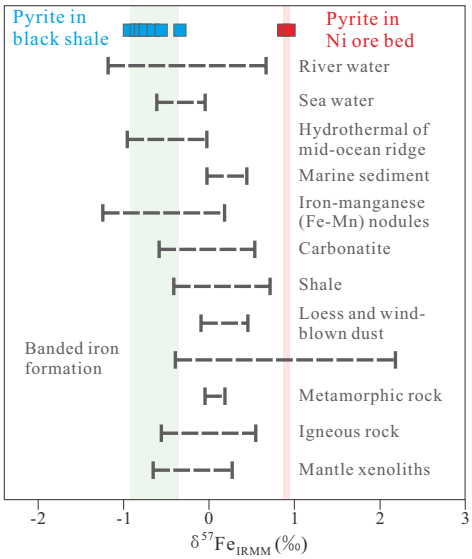

Fig. 4. Comparison of Fe isotopes of pyrite from the Ni ore bed with whole rocks (after Yang et al. (2022)).

8.50) (Fig. 3), indicating that the Ni ore bed deposited under oxic and suboxic conditions. This result is inconsistent with previous researches, which indicate euxinic-close to paleoredox-conditions of the Niutitang black shale (Xia et al., 2020a, 2022; Fu et al., 2021). One of the most significant reasons for this finding is the abnormal enrichment of some metal elements in this ore bed, which were possibly brought by thermal fluids (Han et al., 2017). The paleo environment assessment comparing Ni ore bed and black shale is easily misjudged based on these metal elements, while the comparison among laminae in the Ni ore bed could indicate the environmental changes during the sedimentation of this ore bed.

The Fe isotope of pyrite in the Niutitang black shale and Ni ore bed was analyzed in our earlier research (Yang et al., 2022), and the Fe isotopic values of the Ni ore bed (δ^{57}Fe values range from 0.88‰ to 0.90‰) is obviously higher than that of black shale (δ^{57}Fe values ranging from -0.83‰ to -0.34‰) (Fig. 4). One possible reason is that the effects of deep hydrothermal fluids are different on black shale and Ni ore bed. Another explanation is the redox environmental difference during the deposition of these two sedimentary layers. Thus, changes in the geochemical characteristics and environmental conditions during the deposition of the Ni ore bed are significant for the co-enrichment mechanism of organic matter and Ni. Fortunately, the laminated structure of Ni ore bed and the geochemical variation among different laminae provide a feasible approach to study these changes.

3.2 Characteristics of laminae in Ni ore bed

Some scholars studied the composition of laminae and described the laminae types of Early Cambrian black shale, which mainly include siliceous laminae, calcareous laminae, clay minerals laminae, and organic-rich laminae (Zhu et al., 2019b; Gu et al., 2020). Han et al. (2020) indicated that the Ni ore bed in Early Cambrian black shale consists of Mo mineral laminae, Ni-Mo-Zn sulfides laminae, and Ni-Zn mineral laminae. However, this division did not consider the main components such as quartz, feldspar, calcite, clay, and organic matter. In this study, not only laminae in this Ni ore bed were recognized but also the mineral compositions and element concentrations among different laminae were compared.

The two structures of Ni ore bed is laminated (Figs. 5(a) and 5(b)) and massive (Figs. 5(c) and 5(d)). The former is the research object of this study, with four types of laminae recognized in this ore bed. These are siliceous laminae, calcareous laminae, clay minerals laminae, and organic-rich laminae. Siliceous laminae are mainly composed of quartz and feldspar, and shaped as plate, strip or microwave (Fig. 5). Carbonate minerals such as calcite and dolomite are the dominating components in calcareous laminae, which have smaller amounts in contrast to the others three types of laminae. These are controlled by diagenetic evolution and were not discussed herein. Clay minerals laminae show strip and lens shapes, with illite and montmorillonite being the main components. Organic-rich laminae are black in color and usually interbedded with siliceous laminae or clay minerals laminae.

The element concentrations of siliceous laminae, clay minerals laminae, and organic-rich laminae were measured, and the results can be seen in Table 1. The data indicate that the element concentrations show significant differences among different laminae. Compared with clay minerals laminae and organic-rich laminae, most elements are depleted in siliceous laminae, such as Mg, Al, K, Ca, Ti, V, Cr, Mn, Ni, Sr, Zr, Mo, and Ba. One of the most likely reasons is that clay minerals and organic matter have much stronger adsorption capacity than quartz and feldspar (Fan et al., 2004; Xia et al., 2020b; Ghasemi et al., 2023) and they adsorb a large quantity of elements during the sedimentary and diagenetic stages. Another possible reason is the varied sedimentary conditions of different types of laminae.

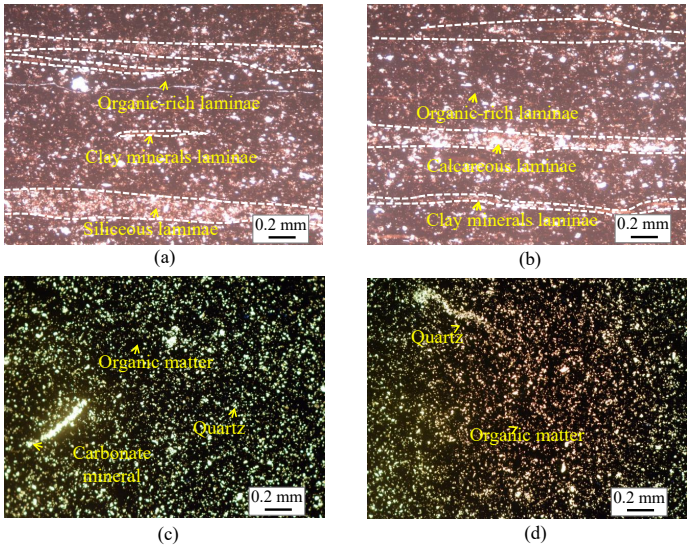

Fig. 5. Characteristics of Late Cambrian organic-rich shale laminae under microscope in the North Guizhou Area. (a) and (b) are laminated structure in shale samples, (c) and (d) are massive structure in shale samples.

3.3 Environmental evolution during laminae generation

The evolution of paleoredox condition, paleoproductivity, and hydrothermal influences during the deposition of the Ni ore bed was analyzed based on the geochemical data of various laminae.

Notably, U and V are redox-sensitive elements that are generally enriched under anoxic and euxinic conditions (Tribovillard et al., 2006; Xia et al., 2022). Unlike U and V, Cr and Th are not redox-sensitive elements and remain insoluble in the marine environment (Ross and Bustin, 2009). The U/Th and V/Cr ratios can indicate oceanic redox conditions. In general, U/Th $>$ 1.25 represents anoxic conditions, and ratios as low as 0.75 represent strongly oxidizing conditions (Wignall and Twitchett, 1996). For V/Cr, $>$ 4.25 indicates anoxic conditions, 4.25-2.00 indicates suboxic conditions, and $<$ 2.00 indicates oxic conditions (Jones and Manning, 1994). The ranges of these ratios for different laminae in the Ni ore bed are shown in Figs. 6 and 7.

The U/Th ratios of clay minerals laminae, organic-rich laminae, and siliceous laminae are in the range of 7.1-833.0 (with an average of 154.9), 1.5-611.9 (with an average of 84.6), and 0.1-87.5 (with an average of 15.5), respectively. These results imply that

1) the study area was dominated by anoxic environments during the sedimentation of clay minerals laminae and organic-rich laminae;
2) during the sedimentation of siliceous laminae, the study area experienced environments ranging from strong oxidizing to anoxic.

These two conclusions are also supported by the V/Cr ratios. The V/Cr ratios of siliceous laminae are 0.9-9.4, indicating laminae depositions under oxic to anoxic conditions.

Biogenic Ba (Ba_{bio}) and biogenic Si (Si_{bio}) are effective proxies used to reconstruct paleoproductivity (Tribovillard et al., 2006; Schoepfer et al., 2015; Moore and Fu, 2018), which can be calculated using the following formulae (Dymond et al., 1992; Ross and Bustin, 2009):

$$Ba_{bio} = Ba_{total} - \left[Al_{total} \times (Ba/Al)_{terrigenous}\right] \quad (1)$$

$$Si_{bio} = Si_{total} - \left[Al_{total} \times (Si/Al)_{terrigenous}\right] \quad (2)$$

where Ba_{total} represents the total amount of barium in the sample, ppm; Al_{total} represents the total amount of aluminum in the sample, ppm; Si_{total} represents the total amount of silica in the sample, ppm; $(Ba/Al)_{terrigenous}$ represents the average Ba/Al ratio of the upper crust; and $(Si/Al)_{terrigenous}$ represents the average Si/Al ratio of the upper crust.

The Ba_{bio} contents of clay minerals laminae, organic-rich laminae, and siliceous laminae are in the range of 4,007.1-54,096.5 ppm (average of 20,181.1 ppm), 1,559.3-37,805.9 ppm (average of 14,561.9 ppm), and 222.2-43,658.0 ppm (average of 7,677.0 ppm), respectively. These results indicate that paleoproductivity during the sedimentation of clay minerals laminae and organic-rich laminae is significantly higher than the sedimentary stage of siliceous laminae. However, the Si_{bio} contents increase from clay minerals laminae (2.3%-39.2%, with an average of 19.4%), through organic-rich laminae (2.3%-91.2%, with an average of 32.5%), to siliceous laminae (1.9%-99.4%, with an average of 41.9%), indicating that siliceous laminae correspond to the highest paleoproductivity among the three types of laminae. The underlying reason will be discussed in the next paragraph.

The lower the Sr/Ba ratios in sediments, the stronger the hydrothermal action is. In general, the Sr/Ba ratios are greater than 1 in normal marine sedimentary rocks, while those lower than 1 indicate the hot water sediment of modern seafloor environments (Jia et al., 2016; Xia et al., 2020a). The Sr/Ba ratios of all samples in the Ni ore bed range from 0.0013

Table 1. Element concentrations of different kinds of laminae in the Ni ore bed.

Laminae types	Clay minerals laminae		Organic-rich laminae		Siliceous laminae	
	Scale	Average	Scale	Average	Scale	Average
Na (ppm)	1,160-28,381	7,343	731-21,385	9,528	100-50,214	9,049
Mg (ppm)	2,808-22,218	9,185	1,141-107,596	16,227	38-31,606	4,502
Al (ppm)	4,515-101,737	55,036	10,858-110,504	70,066	881-86,699	34,641
SiO_2 (%)	13.15-66.05	38.14	6.04-95.36	56.35	3.66-99.66	53.66
P (ppm)	1-94,685	14,072	1-28,437	1,651	1-128,616	5,885
K (ppm)	10,085-41,505	25,276	4,530-48,714	29,424	170-41,648	12,374
Ca (ppm)	710-367,177	60,190	196-170,999	19,977	101-49,162	4,353
Ti (ppm)	835-62,346	7,414	351-37,245	6110	10-16,508	3,513
V (ppm)	330-14,502	2,135	69-1,639	714	3-499	183
Cr (ppm)	55-427	135	18-275	131	2-109	41
Mn (ppm)	9-1,626	254	6-1,943	276	1-1,045	122
Fe (ppm)	8,407-591,276	210,330	5,987-684,095	125,779	242-721,513	243,742
Co (ppm)	3-777	202	2-411	72	1-290	73
Ni (ppm)	313-36,680	5,703	20-1,880	448	1-686	251
Cu (ppm)	11-580	233	9-512	131	2-1,112	149
Zn (ppm)	18-58,047	4,900	12-727	83	1-12,252	686
Sr (ppm)	39-11,648	2,080	23-2,449	469	5-3,122	279
Zr (ppm)	6-909	126	14-239	91	1-93	33
Mo (ppm)	101-25,575	2,594	58-456	205	17-1,815	165
Ba (ppm)	4,147-54,585	20,522	1,627-38,412	14,996	1,946-87,401	11,492
U (ppm)	14-267	70	5-564	93	1-1,272	96

to 1.8922 (Fig. 8). Considering different types of laminae, these ratios of clay minerals laminae, organic-rich laminae, and siliceous laminae are in the range of 0.0023-1.8922 (averaging 0.2584), 0.0035-0.2399 (averaging of 0.0340), and 0.0013-0.1146 (averaging 0.0241), respectively. These results show that

1) hydrothermal activities occurred in study area during the deposition of the Ni ore bed;
2) siliceous laminae experienced much stronger hydrothermal activities than clay minerals laminae and organic-rich laminae.

As shown in Fig. 9, the relationships between the element sets Si+Fe+Mn+P versus Al+Ti+Mg also confirm these results. Moreover, because the effects of hydrothermal activities, Si was partly brought by hydrothermal fluids, a possible reason for the abnormally high Sibio contents in siliceous laminae discussed in the previous paragraph (Jia et al., 2016; Yeasmin et al., 2017).

Moreover, the distribution of laminae in this ore bed follows a somewhat regular pattern. As shown in Figs. 6 and 7, from down to up, the laminae mainly follow two sequences: One of them is from siliceous laminae, through clay minerals laminae, to organic-rich laminae, referred as SCO sets, and the other is from siliceous laminae, through organic-rich laminae, to clay minerals laminae, named as SOC sets. Different sequences/sets imply different environmental evolution histories and will be discussed in the next section.

3.4 Analysis of organo-metal co-enrichment mechanism

The Ni concentrations differ among the three types of laminae in the Ni ore bed. As documented in Table 1, clay minerals laminae have much higher Ni concentration than the other two laminae, with the Ni concentration in the three types ranging from 313 to 36,680 ppm, averaging 5,703 ppm. The upper crustal abundance of Ni is about 44 ppm (McLennan, 2001), so the enrichment factors of Ni in clay minerals laminae can reach 833.64. In contrast to clay minerals laminae, siliceous laminae have much lower Ni concentration, ranging 1-686 ppm (average of 251 ppm). The Ni concentration (from 20 to 1,880 ppm, with an average of 448 ppm) of organic-rich laminae is higher than that of siliceous laminae but lower than that of clay minerals laminae. These results imply that Ni is not ho-

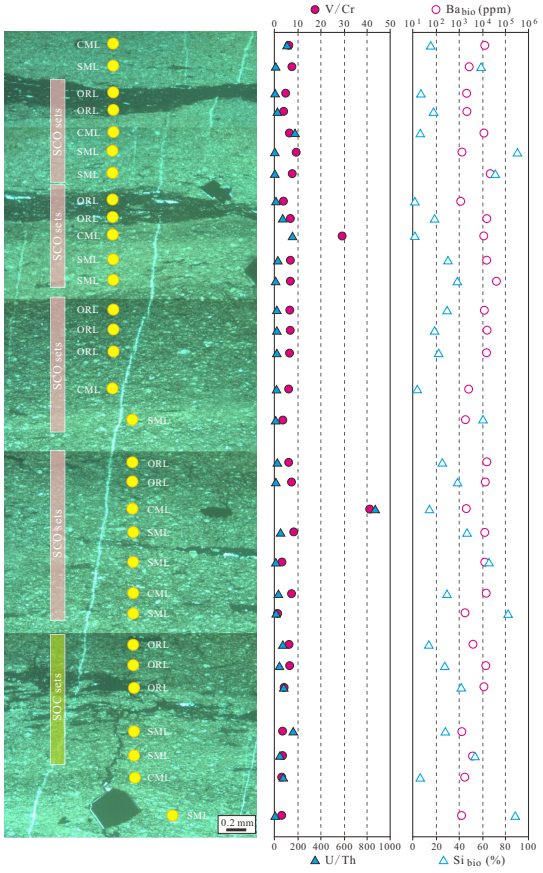

Fig. 6. Variations in paleoproductivity and paleoredox proxies of laminae section 1 of the Ni ore sample.

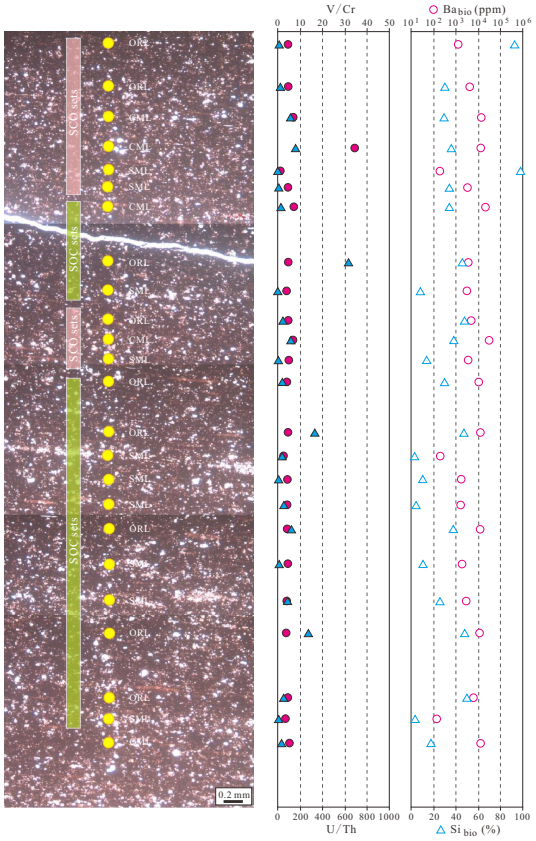

Fig. 7. Variations in paleoproductivity and paleoredox proxies of laminae section 2 of the Ni ore sample.

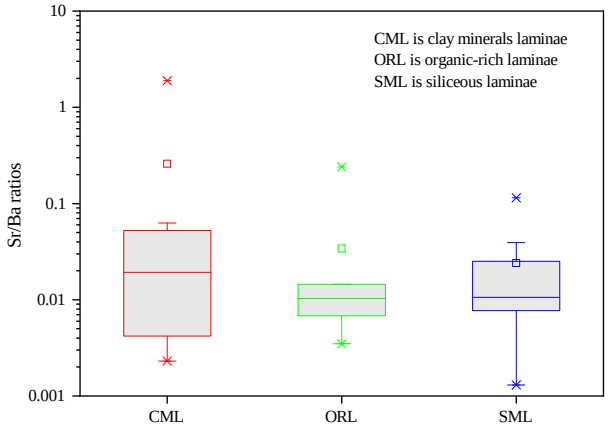

Fig. 8. Sr/Ba ratios of different kinds of laminae.

mogeneously distributed in the Ni ore bed, while it is mainly enriched in clay minerals laminae.

The occurrence of Ni is mainly as independent minerals (such as millerite and mechernichite), isomorphic complexes, and adsorption state (such as adsorbed by clay minerals and organic matter) (Pan et al., 2005; Han et al., 2012; Cao et al., 2013; Shi et al., 2014; Yu et al., 2023). Millerite and mechenichite are of hydrothermal origin (Wu et al., 2007). According to the paleoenvironmental conditions of different types of laminae, clay minerals laminae experienced relatively weak hydrothermal activities but have the highest Ni concentration, implying that independent minerals is not the main occurrence state of Ni in this Ni ore bed. Clay minerals and organic matter have strong Ni adsorption capacity (Zhang et al., 2011; Lehmann et al., 2016; Han et al., 2017), and the adsorption of organic matter to Ni is mainly controlled by aliphatic carbon (Yu et al., 2023).

Adsorption experiments were conducted to reflect the adsorption capacity of clay minerals (such as illite) and organic matter (such as humin), with the results shown in Fig. 10. These data indicate that both illite and organic matter have strong adsorption capacity for Ni, and the adsorption capacity of illite is notably stronger than humin. When illite enters in a standard solution of Ni, it adsorbs more than 80 percent of Ni during the initial 60 minutes. This abnormally strong adsorption capacity of clay minerals for Ni is due to their special structures and compositions; they can adsorb Ni following the principles of ion exchange adsorption and coordination adsorption (Zhang et al., 2017; Liu et al., 2022). Numerous spectroscopic experiments have demonstrated that when silicon is present in the solution at a certain concentration, Ni^{2+} forms new silicate precipitates on the surface of clay minerals at high pH, namely, layered silicates with Ni^{2+} as octahedral cations (Ford et al., 1999; Scheckel and Sparks, 2001; Tan et al., 2017) (Fig. 11). During the deposition stage of laminae, clay adsorbed a large amount of Ni from seawater and pore water than organic matter and the other minerals, and as a result, Ni concentration in clay minerals laminae is higher than in other types of laminae.

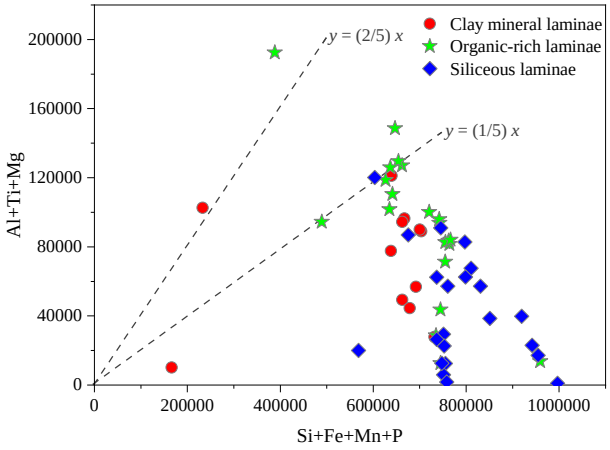

Fig. 9. Relationships between major element sets.

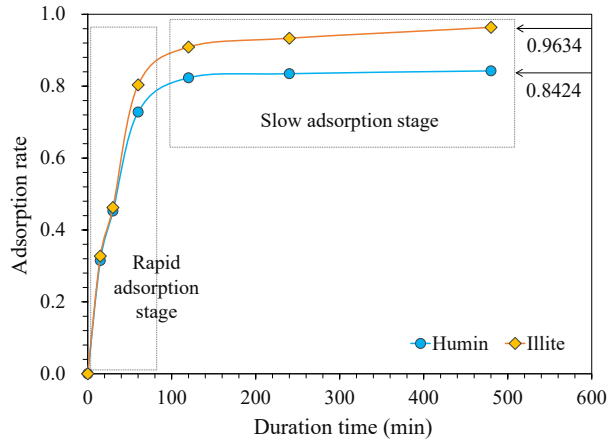

Fig. 10. Adsorption capacity of illite and humin for Ni.

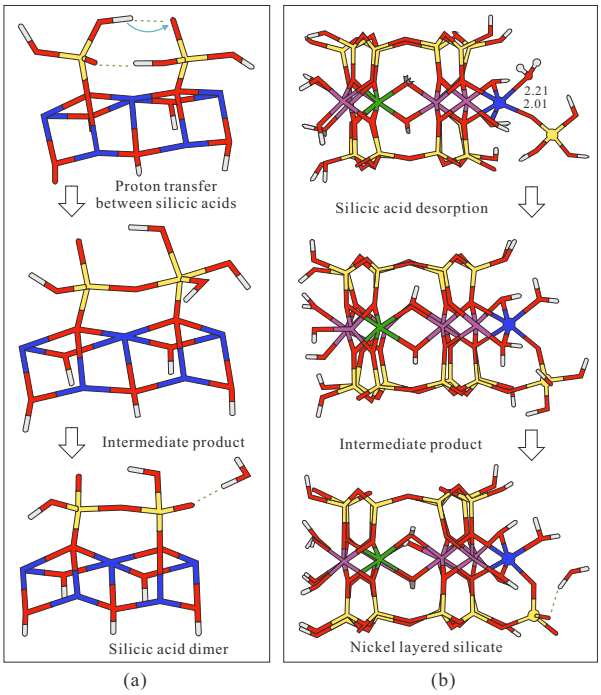

Fig. 11. Forming process of nickel silicate mineral (Dähn et al., 2003; Tan et al., 2017; Zhang et al., 2017). (a) Heavy metal hydroxides first appear as epitaxial growth on the octahedron, and then the hydroxides react with silicic acid to convert into silicates and (b) heavy metals and silicon grow simultaneously on the end faces of clay minerals, directly forming heavy metal layered silicates. Notes: The green dash line means hydrogen bonding; white means H; red means O; green means Mg; yellow means Si; and dark blue means Ni.

Based on the previous discussion, the enrichment mechanisms of Ni and organic matter in the Ni ore bed were shown in Fig. 12. Hydrothermal fluids transported nutrient elements, such as Si, Fe, Mn, P, and Ni, from depth to seawater, resulting in phytoplankton flourishing in the seawater (Yeasmin et al., 2017; Xia et al., 2020a). In addition, organisms such as worms, sponges and bacteria thrived around hydrothermal centers (Jia et al., 2016; Xia et al., 2020a). During this stage, the sedimentary conditions altered from oxic to anoxic, and adequate oxygen in seawater was helpful for the growth of these organisms. Consequently, the paleoproductivity of seawater was increased, and a large amount of organic matter was generated. The generated organic matter was partly oxidized, along with the consumption of oxygen and the reduction of variable valence elements (such as Ni^{3+} was reduced to Ni^{2+}, and S^{6+} and S^{4+} were reduced to S^{2-}) in seawater. Residual organic matter was deposited and preserved in the sediments, associated with sulfide minerals (such as pyrite framboids in Figs. 13(a) and 13(b)). Meanwhile, the conditions of seawater gradually changed from oxic to anoxic or even sulphate environments, and this can be proved by the large amounts of pyrite framboids in organic-rich laminae and clay minerals laminae (Fig. 13). Terrestrial input brought clay minerals into seawater, which adsorbed Ni^{2+} from seawater to generate nickel layered silicate and silicic acid dimers (Fig. 11). Thus, Ni is mainly enriched in clay minerals laminae, and Ni and organic matter are not enriched at the same time. Moreover, clay minerals are closely associated with pyrite framboids in clay minerals laminae (Figs. 13(c) and 13(d)) because of the anoxic to sulphate environments. Following this model, SOC sets would be developed (Fig. 12(a)). In addition, if the terrestrial input occurred earlier than or simultaneously with the hydrothermal event, both would bring nutrients to seawater and then trigger the bloom of phytoplankton. The oxidation of some of the organic matter consumed oxygen, and the residual organic matter was deposited and preserved in sediments under anoxic to euxinic conditions. SCO sets would be generated according to this model (Fig. 12(b)).

The results of this study indicate that the distribution areas of Ni ore bed are more promising for Early Cambrian shale gas exploration and development in the Upper Yangzte Region.

4. Conclusions

1) The Ni ore bed in the Early Cambrian black shale of the Upper Yangzte Region has much higher contents of organic matter and Ni than black shale outside this ore bed. There are four types of laminae in this Ni ore bed, namely, siliceous laminae, calcareous laminae, clay minerals laminae, and organic-rich laminae. Clay minerals

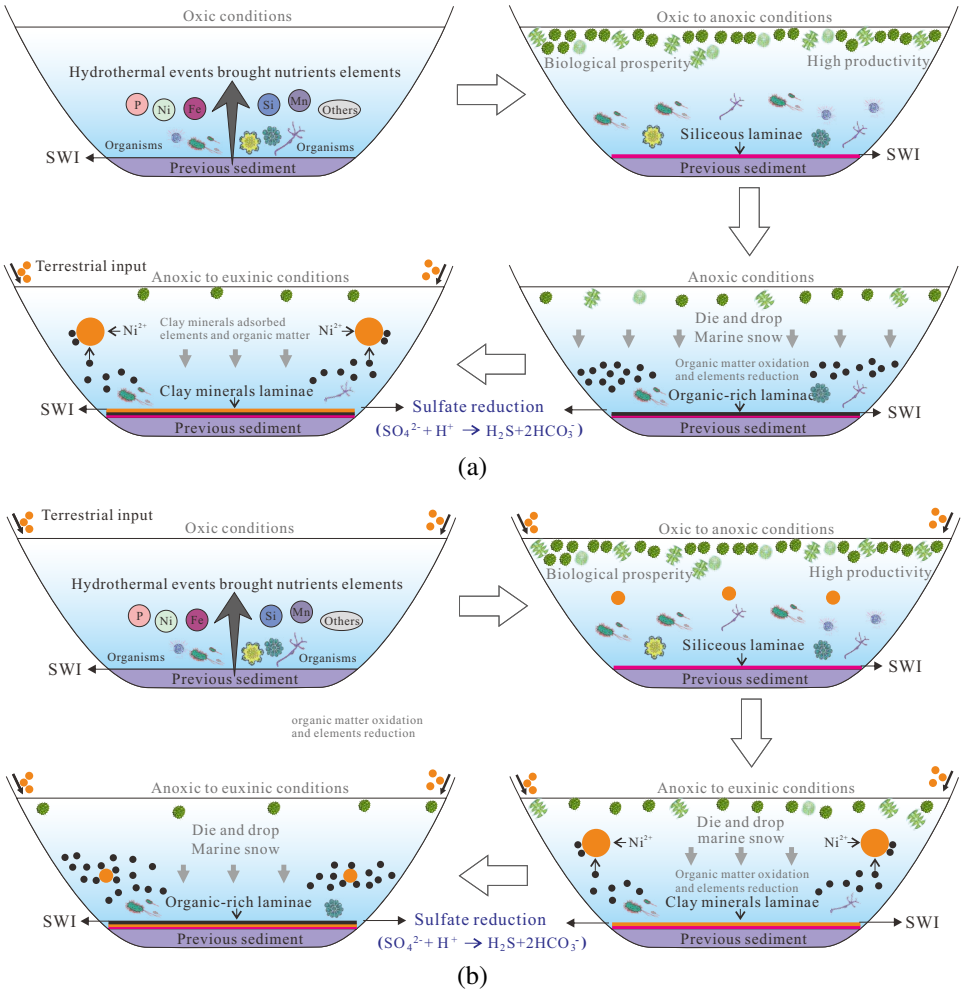

Fig. 12. Schematic model of the enrichment of Ni and organic matter in the study area, where SWI means sediment-water interface. (a) Model for SOC sets and (b) model for SCO sets.

laminae and organic-rich laminae were deposited under anoxic or even euxinic environments, while siliceous laminae were deposited under strong oxidizing to anoxic environments.

2) Both organic matter and Ni has inhomogeneous distribution in the Ni ore bed. Organic matter is mainly distributed in organic-rich laminae, and Ni is mainly enriched in clay minerals laminae. Clay minerals and organic matter have strong adsorption capacity for Ni. Specifically, in contrast to organic matter, clay minerals such as illite have notably stronger adsorption ability for Ni.
3) Even though organic matter and Ni are co-enriched in the Ni ore bed, organic matter and Ni are not enriched at the same time from the perspective of laminae. Hydrothermal events and terrestrial input are key factors affecting the paleoenvironment and laminated structures during the deposition of Ni ore bed.

Acknowledgements

This research was supported by the National Natural Science Foundation Project of China (Nos. 42002166, 42162016 and 42063009), and the Guizhou Provincial Fund Project (No. (2022) ZD005).

Conflict of interest

The authors declare no competing interest.

References

Cao, J., Hu, K., Zhou, J., et al. Organic clots and their differential accumulation of Ni and Mo within early Cambrian black-shale-hosted polymetallic Ni-Mo deposits, Zunyi, South China. Journal of Asian Earth Sciences, 2013, 62: 531-536.

Dähn, R., Scheidegger, A. M., Manceau, A., et al. Structural evidence for the sorption of Ni (II) atoms on the edges of montmorillonite clay minerals: A polarized X-ray absorption fine structure study. Geochimica et Cosmochimica Acta, 2003, 67(1): 1-15.

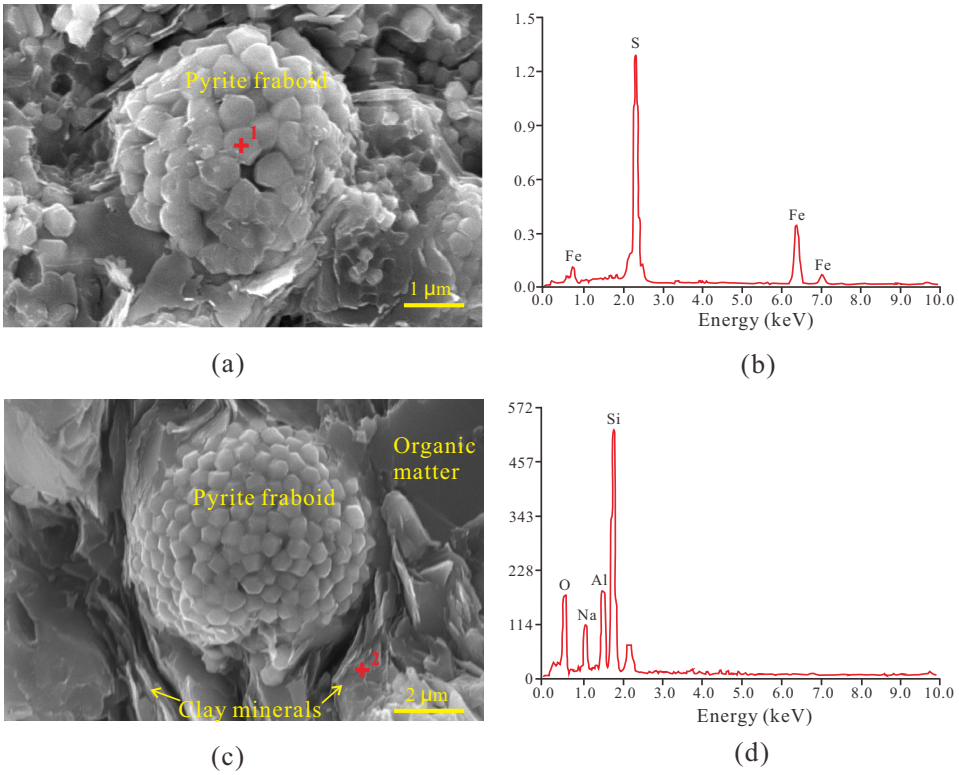

Fig. 13. SEM image and energy spectrum showing the association of organic matter and pyrite framboids. (a) SEM image of organic-rich laminae, (b) energy spectrum at No. 1 red cross, (c) SEM image of clay minerals laminae and (d) energy spectrum at No. 2 red cross.

Dai, C., Zhen, Q., Chen, J., et al. The metallogenic geological background of the Xuefeng Caledonian tectonic cycle in Guizhou, China. Earth Science Frontiers, 2013, 20: 219-225.

Dymond, J., Suess, E., Lyle, M. Barium in deep sea sediments: A geo-chemical proxy for paleoproductivity. Paleoceanography, 1992, 7(2): 163-181.

Fan, D., Zhang, D., Ye, J. Black Rock Series and Related Mineral Deposits in China. Beijing, China, Science Press, 2004. (in Chinese)

Ford, R. G., Scheinost, A. C., Scheckel, K. G., et al. The link between clay mineral weathering and the stabilization of Ni surface precipitates. Environmental Science & Technology, 1999, 33: 3140-3144.

Fu, Y., Zhou, W., Wang, J., et al. The relationship between environment and geochemical characteristics of black rock series of Lower Cambrian in northern Guizhou. Acta Geologica Sinica, 2021, 95: 536-548.

Gao, J., Li, X., Cheng, G., et al. Structural evolution and characterization of organic-rich shale from macroscopic to microscopic resolution: The significance of tectonic activity. Advances in Geo-Energy Research, 2023, 10(2): 84-90.

Ghasemi, M., Tatar, A., Shafiei, A., et al. Prediction of asphaltene adsorption capacity of clay minerals using machine learning. The Canadian Journal of Chemical Engineering, 2023, 101(5): 2579-2597.

Guizhou Geological Survey. In Regional Geology of China: Cambrian. Beijing, China, Geology Press, 2017. (in Chinese)

Gu, Y., Li, X., Yang, S., et al. Microstructure evolution of organic matter and clay minerals in shales with increasing thermal maturity. Acta Geologica Sinica, 2020, 94: 280-289.

Han, S., Hu, K., Cao, J., et al. Mineralogical characteristics of Ni-Mo polymetallic deposits in early cambrian black rock series from southern china. Acta Mineralogica Sinica, 2012, 32: 269-280.

Han, T., Fan, H., Wen, H., et al. Petrography and sulfur isotopic compositions of SEDEX ores in the early Cambrian Nanhua Basin, South China. Precambrian Research, 2020, 345: 105757.

Han, T., Fan, H., Zhu, X., et al. Submarine hydrothermal contribution for the extreme element accumulation during the early Cambrian, South China. Ore Geology Reviews, 2017, 86: 297-308.

Han, T., Zhu, X., Li, K., et al. Metal sources for the polymetallic Ni-Mo-PGE mineralization in the black shales of the Lower Cambrian Niutitang Formation, South China. Ore Geology Reviews, 2015, 67: 158-169.

Hao, F., Zhou, X., Zhu, Y., et al. Lacustrine source rock deposition in response to co-evolution of environments and organisms controlled by tectonic subsidence and climate, Bohai Bay Basin, China. Organic Geochemistry, 2011, 42(4): 323-339.

Hao, F., Zou, H., Lu, Y. Mechanisms of shale gas storage:

Implications for shale gas exploration in China. AAPG Bulletin, 2013, 97(8): 1325-1346.

Hoffman, P. F., Kaufman, A. J., Halverson, G. P., et al. A neoproterozoic snowball earth. Science, 1998, 281: 1342-1346.

Jia, Z., Hou, D., Sun, D., et al. Hydrothermal sedimentary discrimination cri-teria and its coupling relationship with the source rocks. Natural Gas Geoscience, 2016, 27: 1025-1034.

Jones, B., Manning, D. A. C. Comparison of geochemical indices used for theinterpretation of palaeoredox conditions in ancient mudstones. Chemical Geology, 1994, 111: 111-129.

Laranjeira, V., Ribeiro, J., Moreira, N., et al. Geochemistry of Precambrian black shales from Ossa Morena Zone (Portugal): Depositional environment and possible source of metals. Journal of Iberian Geology, 2023, 49: 1-19.

Lehmann, B., Frei, R., Xu, L., et al. Early Cambrian black shale-hosted Mo-Ni and V mineralization on the rifted margin of the Yangtze platform, China: Reconnaissance chromium isotope data and a refined metallogenic model. Economic Geology, 2016, 111: 89-103.

Liang, C., Cao, Y., Liu, K., et al. Diagenetic variation at the lamina scale in lacustrine organic-rich shales: Implications for hydrocarbon migration and accumulation. Geochimica et Cosmochimica Acta, 2018, 229: 112-128.

Li, J., Cai, J. Quantitative characterization of fluid occurrence in shale reservoirs. Advances in Geo-Energy Research, 2023, 9(3): 146-151.

Liu, X., Tournassat, C., Grangeon, S., et al. Molecular-level understanding of metal ion retention in clay-rich materials. Nature Reviews Earth & Environment, 2022, 3: 461-476.

Mao, J., Lehmann, B., Du, A., et al. Re-Os dating of polymetallic Ni-Mo-PGE-Au mineralization in Lower Cambrian black shales of South China and its geologic significance. Economic Geology, 2002, 97: 1051-1061.

McLennan, S. M. Relationships between the trace element composition of sedimentary rocks and upper continental crust. Geochemistry Geophysics Geosystems, 2001, 2: 1021.

Moore, J. K., Fu, W. W., Primeau, F., et al. Sustained climate warming drives declining marine biological productivity. Science, 2018, 359: 1139-1143.

Mou, Y., Xia, P., Zhu, L., et al. Geochemical characteristics of the shale gas reservoirs in Guizhou Province, South China. Arabian Journal of Chemistry, 2024, 17: 105616.

Ning, S., Xia, P., Zou, N., et al. Organic matter pore characteristics of over-mature marine black shale: A comparison of organic fractions with different densities. Frontiers of Earth Science, 2022, 17(1): 310-321.

Och, L. M., Shields-Zhou, G. A., Poulton, S. W., et al. Redox changes in Early Cambrian black shales at Xiaotan section, Yunnan Province, South China. Precambrian Research, 2013, 225, 166-189.

Pan, J., Ma, D., Xia, F., et al. Study on nickel and monlybdenum mineraals in Ni-Mo sulfide layer of the lower cambrian black rock series, northwestern Hunan. Acta Mineralogica Sinica, 2005, 25: 283-288.

Pi, D. H., Liu, C. Q., Shields-Zhou, G. A., et al. Trace and rare earth element geochemistry of black shale and kerogen in the early cambrian niutitang formation in Guizhou province, South China: Constraints for redox environments and origin of metal enrichments. Precambrian Research, 2013, 225, 218-229.

Ross, D. J. K., Bustin, R. M. Investigating the use of sedimentary geochemical proxies for paleoenvironment interpretation of thermally mature organic-rich strata: Examples from the Devonian-Mississippian shales, Western Canadian Sedimentary Basin. Chemical Geology, 2009, 260: 1-19.

Scheckel, K. G., Sparks, D. L. Dissolution kinetics of nickel surface precipitates on clay mineral and oxide surfaces. Soil Science Society Of America Journal, 2001, 65: 685-694.

Schoepfer, S. D., Shen, J., Wei, H., et al. Total organic carbon, organic phosphorus, and biogenic barium fluxes as proxies for paleomarine productivity. Earth-Science Reviews, 2015, 149: 23-52.

Shi, C., Cao, J., Han, S., et al. A review of polymetallic mineralization in lower Cambrian black shales in South China: Combined effects of seawater, hydrothermal fluids, and biological activity. Palaeogeography, 2021, 561: 110073.

Shi, C., Cao, J., Hu, K., et al. New understandings of Ni-Mo mineralization in early Cambrian black shales of South China: Constraints from variations in organic matter in metallic and non-metallic intervals. Ore Geology Reviews, 2014, 59: 73-82.

Tan, X., Liu, G., Mei, H., et al. The influence of dissolved Si on Ni precipitate formation at the kaolinite water interface: Kinetics, DRS and EXAFS analysis. Chemosphere, 2017, 173: 135-142.

Tribovillard, N., Algeo, T. J., Lyons, T., et al. Trace metals as paleoredox and paleoproductivity proxies: An update. Chemical Geology, 2006, 232: 12-32.

Wignall, P. B., Twitchett, R. J. Oceanic anoxia and the end permian mass extinction. Science, 1996, 272(5265): 1155-1158.

Wu, L., Bai, G., Yuan, Z. Mineral Raw Materials Handbook: Mineral Raw Materials of Oil and Gas Energy. Beijing, China, Chemical Industry Press, 2007. (in Chinese)

Xia, P., Fu, Y., Yang, Z., et al. The relationship between sedimentary environment and organic matter accumulation in the niutitang black shale in Zhenyuan, northern Guizhou. Acta Geologica Sinica, 2020a, 94: 947-956.

Xia, P., Hao, F., Tian, J., et al. Depositional environment and organic matter enrichment of early Cambrian black shales in the Upper Yangtze region, China. Energies, 2022, 15: 4551.

Xia, P., Li, H., Fu, Y., et al. Effect of lithofacies on pore structure of the Cambrian organic-rich shale in northern Guizhou, China. Geological Journal, 2020b, 56: 1130-1142.

Xin, B., Zhao, X., Hao, F., et al. Laminae characteristics of lacustrine shales from the Paleogene Kongdian Formation in the Cangdong Sag, Bohai Bay Basin, China: Why do

laminated shales have better reservoir physical properties? International Journal of Coal Geology, 2022, 260: 104056.

Yang, Z., Wu, P., Fu, Y., et al. Coupling of the redox history and enrichment of Ni-Mo in black shale during the early cambrian: Constraints from S-Fe isotopes and trace elements of pyrite, South China. Ore Geology Reviews, 2022, 143: 104749.

Yeasmin, R., Chen, D., Fu, Y., et al. Climatic-oceanic forcing on the organic accumulation across the shelf during the Early Cambrian (Age 2 through 3) in the mid-upper Yangtze Block, NE Guizhou, South China. Journal of Asian Earth Sciences, 2017, 134: 365-386.

Yu, Y., Xia, P., Wang, Y., et al. The Occurrence and Characteristics of Organic Matter in overmature marine shale: A case study of the lower cambrian niutitang formation shale in Guizhou. Journal of Northeast Petroleum University, 2022, 46(4): 1-15.

Yu, Y., Xia, P., Zhong, Y., et al. Effect of adsorption of metal elements Ni and V on the structure of Humin. Rock and Mineral Analysis, 2023, 42(3): 536-547.

Zhang, C., Liu, X., Lu, X., et al. Surface complexation of heavy metal cations on clay edges: Insights from first principles molecular dynamics simulation of Ni (II). Geochimica et Cosmochimica Acta, 2017, 203: 54-68.

Zhang, Q., Hu, X., Zhou, D. Adsorption properties of attapulgite clay of huining for Ni (II). Chemistry & Bioengineering, 2011, 28: 85-87.

Zhang, X., Shu, D., Han, J., et al. Triggers for the Cambrian explosion: Hypotheses and problems. Gondwana Research, 2014, 25: 896-909.

Zhao, W., Guan, M., Liu, W., et al. Low-to-medium maturity lacustrine shale oil resource andin-situconversion process technology: Recent advances andchallenges. Advances in Geo-Energy Research, 2024, 12(2): 81-88.

Zhu, H., Huang, C., Ju, Y., et al. Multi-scale multidimensional characterization of clay-hosted pore networks of shale using FIBSEM, TEM, and X-raymicro-tomography: Implications for methane storage and migration. Applied Clay Science, 2021, 213: 106239.

Zhu, L., Zhang, D., Zhang, J., et al. Geological Theory, Technology and Practice of Paleozoic Passive Marginal Shale Gas in the East of the Upper Yangtze River: The Potential of Shale Gas Resources in Guizhou. Beijing, China, Science Press, 2019a. (in Chinese)

Zhu, M., Yang, A., Yuan, J., et al. Cambrian integrative stratigraphy and timescale of China. Science China: Earth Science, 2019b, 62(1): 25-60.